

# Demonstrating Analog Inference on the BrainScaleS-2 Mobile System

Yannik Stradmann, Sebastian Billaudelle, Oliver Breitwieser, Falk Leonard Ebert, Arne Emmel, Dan Husmann, Joscha Ilmberger, Eric Müller, Philipp Spilger, Johannes Weis, Johannes Schemmel

**Abstract**—We present the BrainScaleS-2 mobile system as a compact analog inference engine based on the BrainScaleS-2 ASIC and demonstrate its capabilities at classifying a medical electrocardiogram dataset. The analog network core of the ASIC is utilized to perform the multiply-accumulate operations of a convolutional deep neural network. We measure a total energy consumption of  $192 \mu\text{J}$  for the ASIC and achieve a classification time of  $276 \mu\text{s}$  per electrocardiographic patient sample. Patients with atrial fibrillation are correctly identified with a detection rate of  $(93.7 \pm 0.7) \%$  at  $(14.0 \pm 1.0) \%$  false positives. The system is directly applicable to edge inference applications due to its small size, power envelope and flexible I/O capabilities. Possible future applications can furthermore combine conventional machine learning layers with online-learning in spiking neural networks on a single BrainScaleS-2 ASIC. The system has successfully participated and proven to operate reliably in the independently judged competition *Pilotinnovationswettbewerb „Energieeffizientes KI-System“* of the German Federal Ministry of Education and Research (BMBF).

**Index Terms**—accelerator, analog computing, DCNN, ECG, inference, low-power, medical, neuromorphic

## I. INTRODUCTION

Inference with convolutional deep neural networks (CDNNs) will become one of the most important tasks for upcoming edge computing devices. Their energy and cost efficiency will determine the complexity of possible applications. This expected demand has induced interest in novel computing architectures – mostly in the form of specialized digital application-specific integrated circuits (ASICs) [1]. An alternative approach to these digital solutions is based on analog computing.

In the area of event-based neuromorphic computing, analog solutions are not new. Over the last four decades several research groups have presented analog neuromorphic architectures, but most of them are not meant for the implementation of CDNNs due to a lack of fast memory access and multi-valued synaptic inputs [2], [3]. The BrainScaleS neuromorphic architecture developed at Heidelberg University is one exception. It supports fully analog vector-matrix multiplication and rectified linear unit (ReLU) functionality, in addition to its normal event-based operation. The only other neuromorphic architecture supporting simultaneously rate- and spike-based models is the digital Tianjic architecture [4].

We present a demonstrator system for the energy-efficient analog inference capabilities of the BrainScaleS-2 architecture (Figs. 1 and 2). It features a combination of a commercially

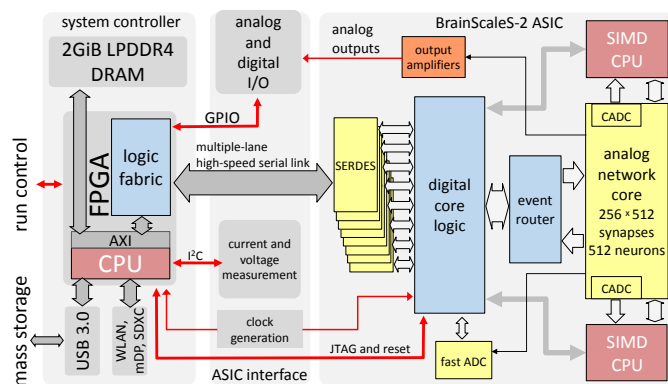


Figure 1. Overview of the BrainScaleS-2 mobile system (from left to right): FPGA-based controller, ASIC interface consisting of two PCBs – the ASIC adapter PCB and the ASIC carrier board –, and BSS-2 ASIC. The system controller provides the USB interface for the USB mass storage device with test and result data as well as the run control handshake signals for the energy measurement protocol of the inference competition.

available field-programmable gate arrays (FPGAs) module and the most recent BrainScaleS-2 ASIC. The FPGA contains an embedded CPU which is used for standalone experiment control and I/O. It is not used during the actual inference process. The logic fabric in the FPGA acts as a memory interface and data format converter for the ASIC. Fig. 1 depicts the three main components of the system:

- a base board consisting of a low-power FPGA with an embedded quad-core microprocessor [5] and 2 GiB of LPDDR4 dynamic random-access memory (DRAM), USB 3.0 (device & host), SDXC, 802.11b/g/n Wi-Fi as well as Bluetooth 4.2 (BLE) communication circuits (see “system controller” in Fig. 1),
- a custom adapter PCB (see “ASIC interface”), interfacing the different connectors of the FPGA board to a single small outline dual in-line memory module (SO-DIMM) connector for the ASIC carrier board,
- the BrainScaleS-2 ASIC directly bonded to a carrier PCB using a SO-DIMM edge connector.

The ASIC uses a bundle of high-speed serial links for bi-directional access to the FPGA fabric. A direct memory access (DMA) controller reads the input data from memory, converts it into input events and sends them to the ASIC. The event router on the ASIC transports the events to inputs of the analog network core, where they are interpreted as the input vector of a vector-matrix multiplication operation. For up to 65 536 signed matrix elements this operation is

All authors contributed equally, see Section V for a detailed description of individual contributions. All authors are with the Kirchhoff-Institute for Physics, Heidelberg, Germany (e-mail: yannik.stradmann@kip.uni-heidelberg.de).

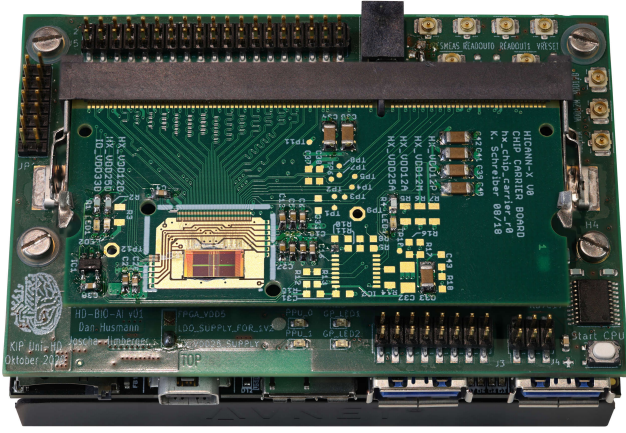


Figure 2. Photo of the BrainScaleS-2 mobile system (from bottom to top): FPGA-based system controller, ASIC adapter PCB, ASIC carrier board with the latest BSS-2 ASIC directly wire-bonded to the PCB. The system has the mechanical footprint of a credit card (84 mm  $\times$  55 mm) at a height of approximately 40 mm. It weighs roughly 155 g with and 70 g without the FPGA’s heatsink respectively.

carried out in parallel within the analog core. The result vector of the vector-matrix multiplication is calculated by the analog neurons, which are configured as linear integrators. Subsequently, the neuron voltages are converted back to the digital domain by a parallel ADC with 8 bit resolution. The ReLU operation can be performed automatically during this conversion. Alternatively, the embedded single instruction, multiple data central processing unit (SIMD CPU) can apply an activation function after digitizing the analog result. These results, representing the output activations of a network layer, are passed to the FPGA fabric and either stored in DRAM or used as inputs for the next layer. This loop is repeatedly executed until all layers have been processed and the final results of the inference operation have been stored in the DRAM memory. Section IV will provide a detailed description of the individual operations involved as well as more insights into the different components of the presented system.

The BrainScaleS-2 mobile system has participated in a competition for low-energy classification of atrial fibrillation (AF) within a medical electrocardiogram (ECG) dataset.<sup>1</sup> We showcase the system’s performance on the training samples of this dataset, consisting of 16 000 data records from the same patient group. The data has been recorded with two channels only, mimicking the signal quality to be expected from consumer-grade medical wearables.

## II. RESULTS

The performance of the presented system has been evaluated by assigning a set of ECG traces to two classes: patients with sinus rhythm and patients showing atrial fibrillation (AF). A description of the used dataset is given in Section I. Mimicking the expected workload in a low-energy edge application, all data has been processed with a batch size of one. To increase the accuracy of all measurements, data was processed in blocks of

<sup>1</sup>Due to the fact that the dataset contains sensitive patient information it is not publicly available.

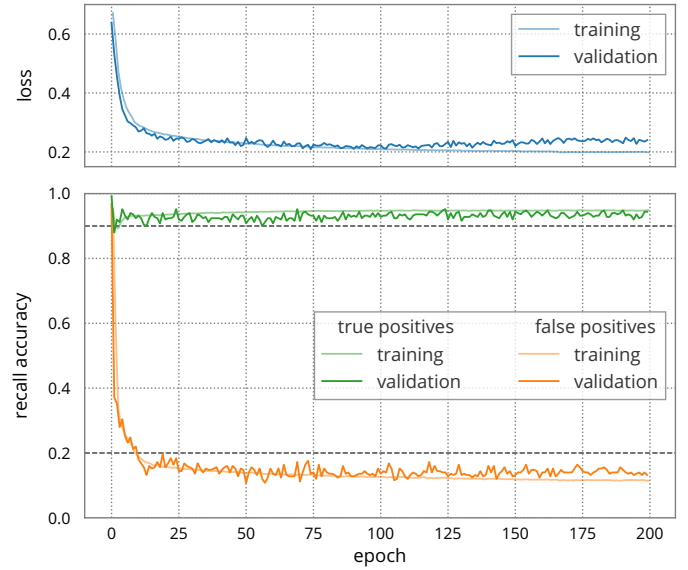


Figure 3. Training and validation metrics of the model presented in Fig. 7 performed with the BSS-2 ASIC. The dashed lines represent the targeted accuracy of 90 % detected atrial fibrillation at a maximum of 20 % false positives. The test set of 500 records was split from the provided ECG dataset prior to training.

500 traces per uninterrupted measurement cycle. For each block, runtime and energy consumption have been measured using the characterization infrastructure described in Section IV-A. The temporal resolution of the power measurements was approximately 294 Hz for sensors on the FPGA base PCB and 4.4 kHz for sensors on the ASIC adapter board.

Classification accuracy has been evaluated by selecting different test sets of 500 records prior to training. Metrics of such a training course on the presented system are shown in Fig. 3. The trained model allows correct classification of  $(93.7 \pm 0.7) \%$  of the AF patients at a false positive rate of  $(14.0 \pm 1.0) \%$ .

Each block of 500 input traces was found to be processed in 138 ms; starting with raw ECG data in the DRAM on the FPGA PCB and ending with binary classification results *ibidem*. Table I gives an overview over the achieved results: The power consumption of the BSS-2 ASIC – where all matrix multiplications take place – is below 15 % of the total system power consumption, leaving significant room for optimization of the auxiliary circuitry. Initial measurements indicate that by disabling all unused components during inference the total power consumption can be reduced by about 50 % to 70 %.

In its current state, the BSS-2 mobile system used a total of 0.78 J for classifying the data of all 500 patients in one evaluation block.

These results have been independently verified by the German Research Center for Artificial Intelligence.

## III. DISCUSSION

We have presented the BSS-2 mobile system as an analog inference platform and demonstrated medical ECG data classification as one possible application. With the shown combination of model, software and hardware, this system classified AF

Table I  
MEASURED RESULTS FOR THE CLASSIFICATION OF 500 RANDOMLY SELECTED ECG TRACES.  
THE TESTED RECORDS HAVE BEEN EXCLUDED FROM TRAINING.

quantity	value	unit
mean power consumption: system	5.6	W
mean power consumption: BSS-2 ASIC	0.7	W
time (500 records)	138	$10^{-3}$ s
classification atrial fibrillation	$93.7 \pm 0.7$	correctly predicted %
classification normal sinus	$86.0 \pm 1.0$	correctly predicted %
total energy	0.78	J
energy FPGA base board	0.35	J
energy ARM central processing unit (CPU)	0.17	J
energy FPGA	0.10	J
energy DRAM (upper limit)	$56 \cdot 10^{-3}$	J
total energy ASIC	$96 \cdot 10^{-3}$	J
energy ASIC IO	$32 \cdot 10^{-3}$	J
energy ASIC analog	$31 \cdot 10^{-3}$	J
energy ASIC digital	$33 \cdot 10^{-3}$	J
total operations in CDNN	$65.875 \cdot 10^6$	Op
BSS-2 ASIC processing speed	$477 \cdot 10^6$	Op/s
BSS-2 ASIC energy efficiency	$689 \cdot 10^6$	Op/J

with a detection rate of  $(93.7 \pm 0.7)\%$  at  $(14.0 \pm 1.0)\%$  false positives. During the inference phase, it achieved 477 MOp/s with a mean power consumption below 6 W, of which below 700 mW are consumed by the BSS-2 ASIC, see Table I. Every patient sample took approximately 276  $\mu$ s to analyze, resulting in an energy efficiency of 84 MOp/J for the full system, or 689 MOp/J for BSS-2 respectively.

The small system is mobile by design and has proven to operate reliable under various environmental conditions. Despite its early prototype stage, it is therefore directly applicable to inference tasks on the edge: The results we have achieved demonstrate that our technology is sufficiently energy efficient such that a hypothetical medical device using it could run on battery while monitoring the health of the patient. Assuming a common CR2032 lithium button battery with an approximated energy content of 200 mA h, the system could perform the inference calculations for detecting atrial fibrillation in two-minute intervals for five years.

The analog inference technology is however not limited to edge applications. Due to its energy efficiency and low cost it is also suitable as a densely packed accelerator in datacenter applications, where the energy cost of inference workloads is expected to become dominant in the upcoming decade [6]–[8]. Our analog solution could be an important step to reduce the energy demands as well as the carbon footprint linked to it.

In addition to the presented multiply-accumulate functionality, BSS-2 is designed to operate as an analog emulator for spiking neural networks (SNNs). To the best of our knowledge, it is the first and only available system to accelerate both, multiply-accumulate operations and SNNs in the analog domain. Due to the stateful nature of the necessary time-continuous operations, multiplexing of analog resources is not possible in most SNN accelerators, therefore limiting the maximum model size to the available hardware resources. In contrast, rate-based stateless operation using our analog neuromorphic core as a parallel vector-matrix multiplier allows for multiplexing hardware resources in time and therefore has the advantage of supporting arbitrarily large model sizes. Such networks are

only limited by the available memory. Most models that are capable of performing real-world tasks, like video analysis or speech translation, need model sizes in the orders of  $10^7$  to  $10^9$  parameters [9]. These network sizes are feasible with the presented system, as neither the hardware platform nor the *hxtorch* software environment described in Section IV-F impose size limitations on the model in use.

The combination of spiking and conventional neural networks on a single substrate therefore greatly widens the application of SNN in edge applications: it allows features to be extracted by conventional high dimensional CDNN layers on multiplexed hardware resources, while sparse spiking layers can simultaneously be used for their final classification. Using the embedded SIMD CPUs, BSS-2 can utilize online learning for the SNN layers and thereby improve classification performance and adapt to environmental changes in the field.

Given its early prototyping stage, the system as well as the BSS-2 chip itself contain a large potential for optimization. Currently, the FPGA is primarily used as a memory controller for the ASIC – functionality that could be incorporated into the chip’s digital core. This would remove the power consumption of the FPGA from the system’s energy balance and could increase the bandwidth between memory and analog core by up to two orders of magnitude.

Furthermore, the speed of the analog calculation has not yet been optimized. While the synapse arrays that perform the multiply-accumulate operation already support 32.8 TOP/s, see (2), the usage of the spike-based neurons for the integration of the summation currents limits the actual speed to approximately 52 GOP/s, see (3). By incorporating specialized circuits for the integration of the synapses’ output currents in the non-spiking operation mode of the ASIC, a single chip could perform well above 10 TOP/s. To reach the maximum throughput of 32.8 TOP/s achievable at the current clock frequency, the I/O bandwidth and the ADC conversion speed have to be increased as well. Higher synaptic operating frequencies could be achieved by splitting the synapse arrays further in smaller banks to shorten the signal wires.

The current area efficiency of the analog MAC in the synapse arrays is

$$\frac{32.8 \text{ TOP/s}}{256 \cdot 512 \cdot 8 \mu\text{m} \cdot 12 \mu\text{m}} = 2.6 \text{ TOP}/(\text{s mm}^2). \quad (1)$$

Since the synapses contain the correlation sensors used only for plasticity in the event-based operation modes, the area efficiency could be increased by a factor of up to three. The shortening of the columns following from the removal of the correlation sensor circuits would also allow a higher operating frequency, further increasing the area efficiency. Values larger than  $10 \text{ TOP}/(\text{s mm}^2)$  seem to be well achievable with the current technology node. Energy efficiency would not increase by the same amount, since making better usage of the synapses' inherent analog computing speed would increase the dynamic power consumption of the I/O circuits and the synapse arrays themselves. Since only a very small part of the power reported in Table I is used for the analog MAC operations, effective total power for the chip performing at its full speed can be estimated to be about  $50 \text{ TOP}/(\text{s W})$ . A fully optimized chip that keeps the analog MAC technology as it has been demonstrated in operation in this paper, while having all circuits optimized for energy and area efficiency, could be expected to perform better than  $100 \text{ TOP}/(\text{s W})$ .

#### IV. METHODS

The described system is the result of tightly coupled interdisciplinary work ranging from machine learning to chip design. The following sections describe different aspects of the BSS-2 mobile system from the perspective of the different technological areas.

##### A. BrainScaleS-2 Mobile System

The hardware system is based on the combination of a FPGA and the BrainScaleS-2 mixed-signal ASIC. It has been introduced in Fig. 1. Further information about the FPGA base board can be found in AVNET [10]. It can be used unaltered in conjunction with the ASIC adapter PCB. In addition to the power monitoring capabilities of the FPGA base board, the individual supply currents of the BrainScaleS ASIC can be monitored by several shunt-based power monitoring integrated circuits (ICs) [11] located on the ASIC adapter PCB. The readout process has been optimized and the ICs were configured for maximum sampling frequency. This enables accurate calculation of the energy consumption by integrating the power samples. Results of these measurements are shown in Section II.

The ASIC adapter PCB provides power supplies, reference voltages and a reference current to the ASIC, which can be accessed via micro-SMT coaxial connectors for debugging purposes. Additional coaxial connectors are available for monitoring the analog outputs from the BSS-2 ASIC. The ASIC itself is directly bonded to a carrier PCB using a zero-insertion force SO-DIMM board edge connector for an optimum combination of simplicity and reliability. Fig. 2 shows the die bonded to the ASIC carrier PCB. The ASIC provides eight independent bi-directional source-synchronous low-voltage differential signaling (LVDS) data channels operated

at up to 2 Gbit/s each. Due to I/O limitations of the FPGA board, only five are routed through the ASIC adapter PCB to the FPGA.

##### B. Neuromorphic ASIC

The BSS-2 neuromorphic ASIC<sup>2</sup> is the key component of the inference system. Fig. 1 shows its major internal functional blocks:

*Analog Network Core:* This is the part of the system performing the inference calculations. It will be described in more detail below.

*Digital Core Logic:* The core control and network logic handles all off-chip communication from the embedded processors and the event router. It also bidirectionally converts between real-time and time-stamped event packets.

*Top and Bottom SIMD CPUs:* The chip includes two custom 32 bit CPUs compatible with the embedded PowerPC instruction set architecture (ISA) [12]. They feature SIMD extensions for fast vector processing. These embedded cores are primarily intended to support learning and plasticity algorithms in SNNs. They can access most of the internal digital resources of the ASIC and – as in this case – serve as experiment controllers.

*Event Router:* Digital logic responsible for the distribution of the real-time vector inputs or spike events to and from the analog network core.

The right side of Fig. 4 shows a layout drawing of the ASIC. The embedded processors are highlighted by the yellow rectangles. The red frame depicts one of the four identical quadrants of the analog core. The left side of the figures illustrates the neuromorphic processing loop through the analog cores, together with the arrangement of neurons and synapses within the quadrants. In the inference experiment, the flow of data is as follows: first, weight data is written into the synapse array via the wide datapaths from the embedded processors. The neurons are configured as linear integrators without any long-term internal dynamics. This is done by setting the appropriate bias values in the analog parameter memories [13]. Inference calculation starts when the network logic transmits the events it has received from the FPGA to the center event routing logic. All neurons are reset to an initial membrane value before the arrival of the first event of the input vector of a vector-matrix multiplication. The event router distributes the events to the synapse drivers, which in turn transmit them into the synapse array. To perform the analog multiplication, the events are converted from binary coding to a pulse length representation. Fig. 5 illustrates the principle of analog computation used for the vector-matrix multiplication. The synapses produce a current proportional to their stored weights  $\omega_x$  for the duration of the input signal they receive from the synapse drivers  $\Delta t$ , thereby performing an analog multiplication of the pulse length representing the input rate value with their stored weights. The input line of the neuron subsequently receives the sum of all

<sup>2</sup>The ASIC has been manufactured in a standard 65 nm CMOS technology. It was conceived and designed at Heidelberg University. The link layer of the high-speed serial links has been developed in collaboration with the TU Dresden, who also contributed the PLL. The fast ADC is a result of a collaboration with the EPFL Lausanne.

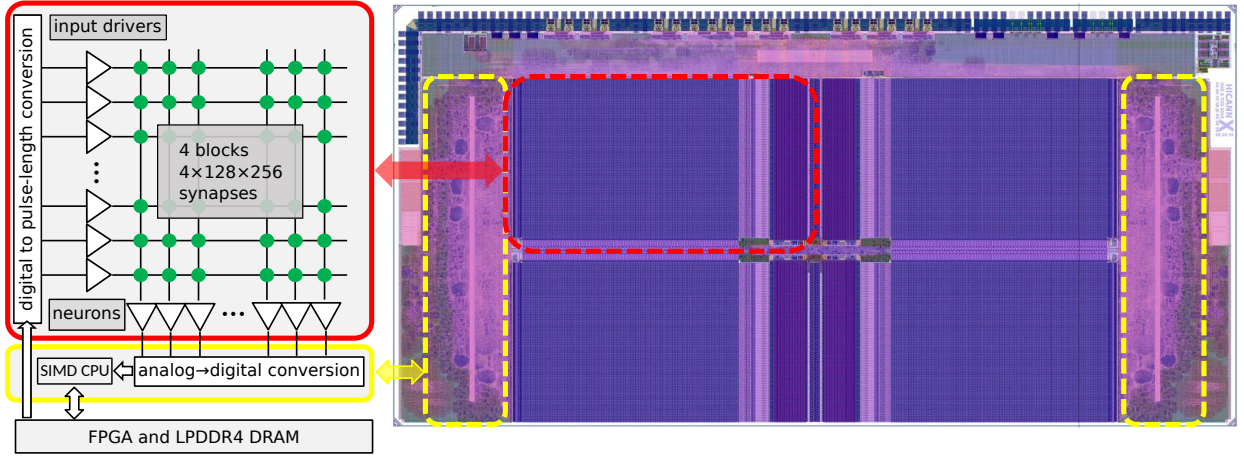


Figure 4. *Left*: internal structure of the BSS-2 ASIC. The analog network core consists of four quadrants, each containing 128 neurons and 128x256 synapses (red). A total of 512 parallel ADC channels allow for readout of various analog parameters by two embedded SIMD processors (yellow). *Right*: position of the described functional units on a layout drawing of the BSS-2 ASIC.

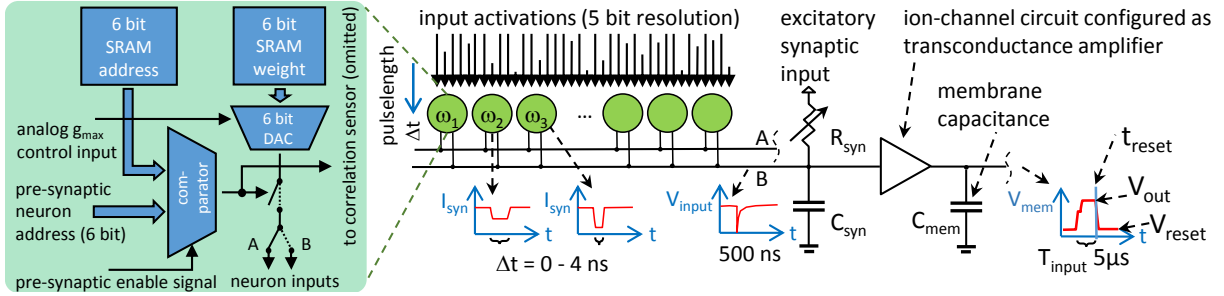


Figure 5. Operation principle of the analog computation: the bottom half depicts the main functional blocks of a synapse circuit. For the inference calculation only the shaded area is used. The top half shows the analog operations taking place: each synapse generates a current pulse  $I_{syn}$  in response to a pre-synaptic input event. During the calculation period  $T_{input}$  they are integrated on the membrane capacitance. The final voltage  $V_{out}$  of a single neuron represents the result of the analog dot-product calculation.

output currents generated by the synapses within a vertical column. For reasons of printing space the column is shown horizontally in the figure.

Each synapse array can process back-to-back activations within 8 ns, the maximum continuous input data rate is therefore 125 MHz. There are  $256 \times 512$  synapses altogether, which can all simultaneously process input activations at the full input data rate. This equals to a maximum of

$$125 \text{ MHz} \cdot 256 \cdot 512 \cdot 2 \text{ Op} = 32.8 \text{ TOP/s}, \quad (2)$$

counting multiplication and addition as individual operations, see Fig. 5. A transconductance amplifier in each neuron generates a current equivalent to the charge received from the synapses. Each column's current is integrated on the membrane capacitance of its associated neuron circuit. Each neuron has two separate inputs for excitatory (A) and inhibitory (B) synaptic inputs. For the inference calculation, they are used to represent positive and negative weight values.

The full integration cycle within the neurons, including the necessary time to reset the neuron membrane voltages, takes about 5  $\mu$ s. This reduces the MAC frequency to 200 kHz and the resulting speed to approximately

$$\frac{1}{5 \mu\text{s}} \cdot 256 \cdot 512 \cdot 2 \text{ Op} \approx 52 \text{ GOP/s} \quad (3)$$

(see Section III). After all input events have been received by the synapses, the membrane voltages of the neurons represent the result of the vector-matrix multiplication. The parallel analog-to-digital converter between the synapse array and the embedded processor can also digitize the membrane voltages. For ReLU operation, its programmable input range can be set in a way that its minimum input value represents the initial reset voltage  $V_{reset}$  the neurons have been initialized to, thereby cutting of the negative branch of the neurons transfer function. After the ADC conversion is completed, the result of the vector-matrix multiplication is transferred into a vector register of the processor and the array is ready for the next operation. For more details of the BrainScaleS-2 architecture refer to Schemmel, Kriener, Müller, *et al.* [14], Aamir, Stradmann, Müller, *et al.* [15], Schemmel, Billaudelle, Dauer, *et al.* [16], Billaudelle, Stradmann, Schreiber, *et al.* [17], and Friedmann, Schemmel, Grübl, *et al.* [18], for the rate-based operation mode see Weis, Spilger, Billaudelle, *et al.* [19] and Weis [20].

### C. FPGA Fabric

Fig. 6 depicts the internal structure of the logic fabric. Main components are the link control and physical layer that implement the high-speed serial links to the ASIC. The playback-buffer contains a list of commands to send to the

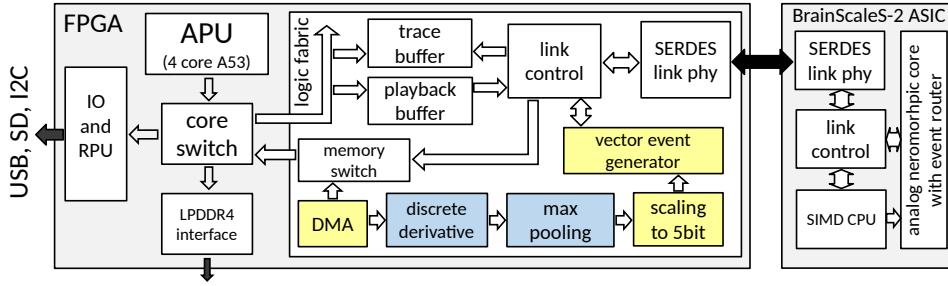


Figure 6. Block diagram of the major functional units of the FPGA, the part inside the logic fabric has been realized as custom RTL in SystemVerilog. The DMA controller, preprocessing chain elements and vector event generator create the input activation events representing the vector in the vector-matrix multiplication. Some of the preprocessing (blue) is problem-specific for the medical ECG dataset. To the right side the major blocks of the BSS-2 ASIC are shown as well to illustrate the complete communication path from the embedded SIMD CPUs to the DRAM memory. The arrows denote the control flow direction from initiator to follower of the internal (hollow) and external (filled) data buses shown in the figure.

ASIC, while the trace buffer collects events sent back from the ASIC. Memory-mapped write and read commands can also be issued from the ASIC to the FPGA. This allows the SIMD CPUs to access the DRAM memory connected to the FPGA via a memory switch.

The DMA controller is programmed by the SIMD CPU on the ASIC to transfer the raw signal data, an ECG trace composed of 12 bit values, from memory. The ASIC requires specially formatted event data packets encoding 5 bit input activations for the vector-matrix multiplication. This demands a preprocessing chain inside the FPGA, which is problem-specific to some extent. Its function will be explained in Section IV-D. After the raw signal data is converted into 5 bit values, the vector event generator attaches an event address from a lookup table. This event is sent to the ASIC via the serial links. In the ASIC the attached addresses are used to forward the events to their target inputs of the analog neuromorphic core. The use of a lookup table inside the FPGA allows arbitrary mapping of input vector elements onto the synapse matrix. During the inference process the SIMD CPU inside the ASIC synchronizes the vector event generator inside the FPGA using multiple handshake signals to control the timing of the sent events.

The selected FPGA contains four 64 bit ARM processor cores in addition to the logic fabric [5]. They do not participate in the inner loop of the inference calculation and only perform initialization and calibration procedures beforehand.

#### D. Model

The model selection for the ECG classification was governed by minimizing runtime to optimize the energy efficiency while achieving reasonable classification accuracy using the available accelerator. As a trade-off between accuracy and model complexity, a minimum AF detection rate of 90 % at a maximum of 20 % false positives was targeted.

Due to the nature of our processing hardware, the best results in both aspects, energy efficiency and detection accuracy, can be obtained with a large batch size, i.e., processing the dataset as a whole. Larger networks promise superior classification accuracy, but require reconfiguration of the ASIC during execution. Since the reconfiguration is only needed once per batch, with a larger batch size its time penalty diminishes. The

best accuracies achieved with larger networks on the BSS-2 ASIC have been 95.5 % for AF with 8.0 % false-positives [21]. However, sequential processing of the data, i.e., batch size one, is preferable for low-energy edge applications. Evaluation of network models showed that even a smaller network that fits on a single chip and does not require reconfiguration can achieve decent accuracy.

It is very plausible that, given the nature of the ECG data, a hand-crafted signal-processing based algorithm running fully in the FPGA would also be feasible. Nevertheless, we aimed to perform as much processing as possible in an automatically trained CDNN, since this approach is also suitable for different kinds of data. As a result, the developed model architecture and software integration for BSS-2 can be easily applied to other machine learning tasks and larger networks, as already demonstrated for human activity recognition [22] and the MNIST handwritten digits [19]. It has been further demonstrated that our trained model can be directly applied to other ECG datasets used in the machine learning community without any manual changes [21].

The BSS-2 ASIC supports acceleration of both spike-based and rate-based neural networks. The main advantage of the spike-based operation modes are the possibility to combine it with online, biologically inspired, learning algorithms executed fully on-chip. Some early tests with spike-based processing concepts to classify AF have been performed on the hardware [20]. For future network concepts, the combination of both modes seems promising. For this publication, however, the BSS-2 ASIC is configured to be used as an analog inference accelerator for vector-matrix multiplication in rate-based CDNNs. A decisive advantage of this mode is that it is based on a stateless network, is very generic and supports multiplexing of larger networks.

The network as used in this publication is depicted in Fig. 7. The model operates on 13.5 s of the 120 s long ECG records, as this has turned out to be sufficient for classification of AF. To the left, the graph of the model is shown. It consists of one convolutional and two linear layers. The small size of the network allows it to be completely realized on the ASIC. The mapping of the network layers to the two halves of the BSS-2 ASIC is shown in the right side of the figure. The ReLU and the final argmax operations are preformed in the embedded SIMD

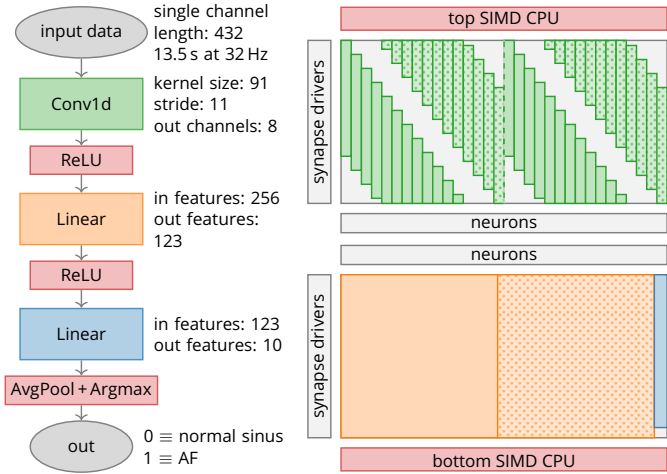


Figure 7. Layer structure (left) and on-chip arrangement (right) of the used deep convolutional neural network model. The convolutional layer (green) is processed in the upper synapse array, the identical weight is arranged 32 times on the substrate to enable parallel processing. All ReLUs (red) are performed in digital logic by the two SIMD CPUs. The further processing takes place on the lower synapse array with a fully connected layer and 123 hidden neurons (orange). To ensure efficient use of the substrate, it is divided into two parts and placed side by side. The dotted part of the layer receives the second half of inputs at the same time and is processed in parallel. The actual classification is then achieved in the last layer (blue) with 10 neurons on the right, which are combined into two logical neurons by average pooling, effectively reducing analog noise.

CPUs after digital readout of the analog neuron membrane voltages.

The ASIC operates on positive activations with 5 bit resolution. Since the raw data samples as input for the inference calculation are provided as 12 bit values with quite large dynamic range, some preprocessing is required. Fig. 8 illustrates the performed steps. To avoid unnecessary data movement, the preprocessing is done in the FPGA fabric by a custom processing chain. In the first step of the preprocessing, a discrete derivative of the original signal is calculated to suppress the large baseline fluctuations of the signal. In a second step, the data rate is reduced by calculating the difference between the maximum and the minimum of 32 samples. This operation is performed with a stride of 16, resulting in an output sample rate of 32 Hz. The resulting samples are quantized to 5 bit and used as inputs to the analog vector-matrix multiplications performed within the ASIC.

Considering the target of maximum energy efficiency, the chosen network is optimized to the resources provided by the BSS-2 ASIC. The calculations in its convolutional first layer can be performed fully in parallel, as well as those in the second and third layers. The total time for processing of all layers of the network is in the order of microseconds. The system has to be active only during this very small time window, plus a few microseconds at the beginning and the end to transfer data back and forth.

### E. Training

Training relies on the proven backpropagation algorithm for CDNNs [24]. In order to fast-prototype and train the network described in Section IV-D, a mathematical abstraction of the

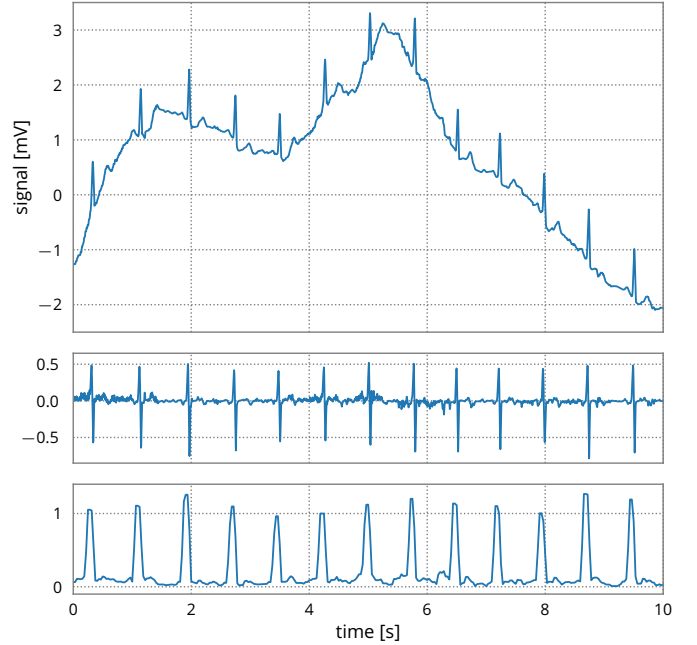


Figure 8. Preprocessing steps performed in the FPGA fabric (from top to bottom): The raw, i.e. unprocessed, input sample is transformed by taking a discrete derivative to reduce baseline fluctuations. Subsequent maximum-minimum difference pooling reduces the sample rate and provides positive activations, which form the final input signal to the CDNN in the ASIC. Original data taken from Clifford, Liu, Moody, *et al.* [23].

hardware operations was implemented on top of PyTorch [25] in *hxtorch* [22]. Incorporating hardware related constraints, like fixed-pattern noise and limited dynamic range, it enables training initial models off-chip and provides gradient information for the backward-path when training on hardware [21]. Final model parameters as presented in Section II were trained on the real ASIC from scratch with no pre-training in software. The provided training data was randomly split into local training and validation datasets. To prevent overfitting validation data was never used during training. We follow the in the loop paradigm [26]: The forward path is evaluated using real hardware whereas the backwards path and parameter updates are calculated on the host computer using *hxtorch*. Tensor data structures are seamlessly converted to hardware resolution and back. Data partitioning and experiment control is handled by both on-chip SIMD CPUs (see Section IV-F). To the user, the training procedure is completely embedded within PyTorch. To increase robustness and decrease sensitivity to hardware variations, we replace the average pooling in the last layer by a max pooling operation during training. Training ends when no substantial improvement is observed between training epochs.

### F. Software

Although the energy efficiency of the inference task relies on analog computing and digital support infrastructure, software plays an essential role. Similarly to other digital hardware platforms software is an essential component to make complex hardware systems accessible to users [27], [28]. In each phase – from hardware commissioning, model design, training to validation phase – users can take advantage from a software

environment that provides appropriate abstraction levels, access to hardware debugging information as well as robust and transparent platform operation. For the BSS-2 architecture, – and, in particular the mobile system – we provide software support for different system aspects:

*User Interface:* The PyTorch toolkit [25] is a commonly used workhorse in the field. Particularly, it simplifies many aspects of CDNN modeling. We developed a custom extension for PyTorch, *hxtorch* [22], [29], providing support for the BSS-2 architecture.

*Training:* Forward propagation is dispatched to the BSS-2 ASIC while backward propagation is performed in software. Hence, *hxtorch* enables using the BrainScaleS-2 system as an inference accelerator in PyTorch while adopting a hardware-in-the-loop-based training approach. The trained model can be serialized, stored to disk and used in an *standalone inference mode* to increase energy efficiency. In addition, a “mock mode” enables the simulation of certain hardware properties in software. This facilitates migrating from the training of a pure software model to a hardware-in-the-loop-based training.

*Hardware Resources:* *hxtorch* provides support for the execution of neural network graphs on an arbitrary number of BSS-2 ASICs. Individual layers are partitioned into chip-sized chunks and executed either in parallel, serially or in the appropriate mixture needed to fit on the available hardware resources. Finally, each ASIC receives and executes a stream of instructions and data.

*Data-Flow Graph Execution:* Internally, *hxtorch* model layers build up a data-flow graph. A just-in-time (JIT) compiler traverses the graph and partitions individual layers into chunks fitting onto the available hardware resources. Partitioned layers are converted into configuration data and corresponding control flow statements; Both of which are transferred to the BSS-2 hardware system and result data is read back. Regarding control flow, the hardware execution engine supports two modes: the first mode uses the FPGA to handle control flow; the second mode, which is also largely used in the standalone inference mode, hands over the control flow to the embedded SIMD CPUs of the ASIC.

*Memory Management:* Data input as well as output locations are precomputed by the BSS-2 software stack allowing for static memory management on the system. The SIMD CPUs use the communication link to the FPGA to program the DMA engine inside the FPGA to automatically deliver the input activations from DRAM to the analog processing cores. Analog operation results are read out by the processors, either held in static random-access memory (SRAM) for temporary data, or stored back into DRAM for output data.

*Standalone Inference Mode:* The BSS-2 software layers are written in C++ and provide faster execution speeds compared to an interpreted top-level language such as Python. To create a lightweight inference flow for the energy measurements, a stand-alone version of the *hxtorch* hardware graph executor was developed. This executor is implemented as a standalone binary and builds upon the same internal software layers and data formats as the *hxtorch* extension. In contrast to the JIT-based execution flow, the standalone inference mode requires control flow to be handled by the embedded SIMD CPUs. The

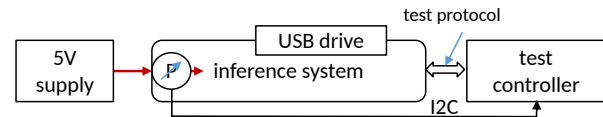


Figure 9. Evaluation setup for the BSS-2 mobile system: power is supplied using a single 5V supply, the power delivery of which is measured at the system’s input. Test data can optionally be read from and results can be written back to a USB mass storage device. GPIO pins are available for orchestrating different phases of the experiment from an optional external controller.

processors process a instruction stream representing: data load and store operations, trigger operations for delivery of input activations from the FPGA, reading out the neuron membrane values, or performing digital operations that are not supported by the analog substrate.

*Embedded System Environment:* The BSS-2 mobile system includes a Linux environment<sup>3</sup> running on an embedded ARM64 processor. We take advantage of a fully containerized software environment based on singularity [30] and spack [31] to provide a cross-compiler environment on the host computer as well as on the embedded Linux system. Standard Linux drivers (xHCI, mass storage, FAT32) are used to readout test data from an USB mass storage device; additionally, support for USB-based Ethernet networking hardware is enabled to facilitate remote system usage. An experiment execution service enables users to run Python-based interfaces on host computers that exchange serialized experiment configurations and result data with the mobile system.

Details of *hxtorch* and the lower levels of the BSS-2 software stack are described in Spilger [29] and Müller, Mauch, Spilger, *et al.* [32].

### G. Scope and Evaluation Procedure

As introduced in Section I, the BSS-2 mobile system participated – as project HD-BIO-AI – in a competition for low-energy classification of ECG data that has been organized by the German Federal Ministry of Education and Research (BMBF). To ensure comparability of the contenders, all competing designs had to adhere to a common interface for experiment orchestration. It specifies a total of four phases for system initialization, transfer of input data from a USB mass storage device to the internal DRAM, inference and the transfer of classification results back to the attached storage device. Final measurements were taken for multiple blocks per 500 ECG traces. Fig. 9 depicts this evaluation setup. The included Inter-Integrated Circuit (I<sup>2</sup>C) chain is not part of this protocol and can optionally be used for fine-grained power measurements of the sensors described in Section IV-A. All official measurements for comparing the competition’s contenders were conducted with off-system equipment supplied by the external power supply.<sup>4</sup>

<sup>3</sup>Petalinux; the build flow of the embedded Linux distribution is provided by the FPGA manufacturer.

<sup>4</sup>The the experiment interface has been designed and final evaluation measurements were taken at the German Research Centre for Artificial Intelligence (DFKI) Kaiserslautern under the direction of Prof. Dr. Hans Dieter Schotten.

## V. CONTRIBUTIONS

Yannik Stradmann directed the development and modeling efforts for the presented experiment and hardware setup. He contributed to all components. Sebastian Billaudelle contributed to the chip design, chip commissioning and implementation of the experiment. Oliver Breitwieser contributed to the software stack, is a main developer of the preemptive experiment scheduling service and contributed to modeling and model verification. Falk Ebert is a main contributor to the energy measurement system. Arne Emmel developed and implemented the model, designed the preprocessing, adapted the training to the hardware platform and contributed to the software integration. Dan Husmann developed the ASIC adapter PCB. Joscha Ilmberger is the main system developer contributing to PCB design, porting of the FPGA design to the new platform and adding functionality such as preprocessing and the vector event generator. Eric Müller is the lead developer and architect of the BSS-2 software stack; he commissioned the embedded platform, ported the software development environment as well as the BSS-2 software stack to the embedded FPGA platform. Philipp Spilger is the main developer of the software for the non-spiking operation mode of the BSS-2 ASIC and a contributor to the software stack. Johannes Weis is the main developer of calibration routines for the analog network core, commissioned the first non-spiking experiments on the hardware platform and contributed to the model. Johannes Schemmel is the lead designer and architect of the BSS-2 neuromorphic system. He wrote the initial version of the paper. All authors contributed to and edited the final manuscript.

## ACKNOWLEDGMENTS

The authors wish to thank all present and former members of the Electronic Vision(s) research group contributing to the BrainScaleS-2 neuromorphic platform. The development of the presented ECG classification system has been funded by the German Federal Ministry of Education and Research (BMBF) under grant number 16ES1127 as part of the *Pilotinnovationswettbewerb „Energieeffizientes KI-System“*. It is built upon work funded by the EU (H2020/2014-2020: 720270, 785907, 945539 (HBP)) and the Lautenschläger-Forschungspreis 2018 for Karlheinz Meier.

## REFERENCES

- [1] Coral. (Aug. 2020). “Edge TPU performance benchmarks”, [Online]. Available: <https://coral.ai/docs/edgetpu/benchmarks/>.
- [2] S. Moradi, N. Qiao, F. Stefanini, and G. Indiveri, “A scalable multicore architecture with heterogeneous memory structures for Dynamic Neuromorphic Asynchronous Processors (DYNAPs)”, *IEEE Trans. Biomed. Circuits Syst.*, vol. 12, no. 1, pp. 106–122, 2018.
- [3] B. V. Benjamin, P. Gao, E. McQuinn, S. Choudhary, A. R. Chandrasekaran, J.-M. Bussat, R. Alvarez-Icaza, J. V. Arthur, P. A. Merolla, and K. Boahen, “Neurogrid: A mixed-analog-digital multichip system for large-scale neural simulations”, *Proceedings of the IEEE*, vol. 102, no. 5, pp. 699–716, 2014.
- [4] J. Pei, L. Deng, S. Song, M. Zhao, Y. Zhang, S. Wu, G. Wang, Z. Zou, Z. Wu, W. He, F. Chen, N. Deng, S. Wu, Y. Wang, Y. Wu, Z. Yang, C. Ma, G. Li, W. Han, H. Li, H. Wu, R. Zhao, Y. Xie, and L. Shi, “Towards artificial general intelligence with hybrid Tianjic chip architecture”, en, *Nature*, vol. 572, no. 7767, pp. 106–111, Aug. 2019.
- [5] Xilinx, *Zync UltraScale+ MPSoC Data Sheet*, 2019. [Online]. Available: [https://www.xilinx.com/support/documentation/data\\_sheets/ds891-zynq-ultrascale-plus-overview.pdf](https://www.xilinx.com/support/documentation/data_sheets/ds891-zynq-ultrascale-plus-overview.pdf).
- [6] J. Park, M. Naumov, P. Basu, S. Deng, A. Kalaiah, D. Khudia, J. Law, P. Malani, A. Malevich, S. Nadathur, J. Pino, M. Schatz, A. Sidorov, V. Sivakumar, A. Tulloch, X. Wang, Y. Wu, H. Yuen, U. Diril, D. Dzhulgakov, K. Hazelwood, B. Jia, Y. Jia, L. Qiao, V. Rao, N. Rotem, S. Yoo, and M. Smelyanskiy, *Deep Learning Inference in Facebook Data Centers: Characterization, Performance Optimizations and Hardware Implications*, 2018. arXiv: 1811.09886 [cs.LG].
- [7] J. Dongarra, S. Gottlieb, and W. T. C. Kramer, “Race to Exascale”, *Computing in Science & Engineering*, vol. 21, no. 1, pp. 4–5, 2019. DOI: 10.1109/MCSE.2018.2882574.
- [8] J. X. Chen, J. Carver, S. Gottlieb, D. E. Post, and B. I. Schneider, Eds., *Computing in Science & Engineering* vol. 21, 1 2019, *Race to Exascale: Race to Exascale*.
- [9] R. Aharoni, M. Johnson, and O. Firat, “Massively Multilingual Neural Machine Translation”, in *Proceedings of the 2019 Conference of the North American Chapter of the Association for Computational Linguistics: Human Language Technologies, Volume 1 (Long and Short Papers)*, Minneapolis, Minnesota: Association for Computational Linguistics, Jun. 2019, pp. 3874–3884. DOI: 10.18653/v1/N19-1388. [Online]. Available: <https://www.aclweb.org/anthology/N19-1388>.
- [10] AVNET, *Ultra96-V2*, 2020. [Online]. Available: [http://zedboard.org/sites/default/files/product\\_briefs/5365-pb-ultra96-v2-v10b.pdf](http://zedboard.org/sites/default/files/product_briefs/5365-pb-ultra96-v2-v10b.pdf).
- [11] Texas Instruments, *INA219 Zero-Drift, Bidirectional Current/Power Monitor With I2C Interface*, 2020. [Online]. Available: <https://www.ti.com/lit/ds/symlink/ina219.pdf>.
- [12] PowerISA, “PowerISA Version 2.06 Revision B”, Power.org, Specification, Jul. 2010. [Online]. Available: <http://www.power.org/resources/reading/>.
- [13] M. Hock, A. Hartel, J. Schemmel, and K. Meier, “An analog dynamic memory array for neuromorphic hardware”, in *Circuit Theory and Design (ECCTD), 2013 European Conference on*, Sep. 2013, pp. 1–4. DOI: 10.1109/ECCTD.2013.6662229.
- [14] J. Schemmel, L. Kriener, P. Müller, and K. Meier, “An Accelerated Analog Neuromorphic Hardware System Emulating NMDA- and Calcium-Based Non-Linear Dendrites”, in *2017 International Joint Conference on Neural Networks (IJCNN)*, 2017, pp. 2217–2226. DOI: 10.1109/IJCNN.2017.7966124.
- [15] S. A. Aamir, Y. Stradmann, P. Müller, C. Pehle, A. Hartel, A. Grübl, J. Schemmel, and K. Meier, “An

- Accelerated LIF Neuronal Network Array for a Large-Scale Mixed-Signal Neuromorphic Architecture”, *IEEE Transactions on Circuits and Systems I: Regular Papers*, vol. 65, no. 12, pp. 4299–4312, Dec. 2018, ISSN: 1549-8328. DOI: 10.1109/TCSI.2018.2840718.
- [16] J. Schemmel, S. Billaudelle, P. Dauer, and J. Weis, “Accelerated Analog Neuromorphic Computing”, *arXiv preprint*, 2020. arXiv: 2003.11996 [cs.NE].
- [17] S. Billaudelle, Y. Stradmann, K. Schreiber, B. Cramer, A. Baumbach, D. Dold, J. Göltz, A. F. Kungl, T. C. Wunderlich, A. Hartel, E. Müller, O. Breitwieser, C. Mauch, M. Kleider, A. Grübl, D. Stöckel, C. Pehle, A. Heimbrecht, P. Spilger, G. Kiene, V. Karasenko, W. Senn, M. A. Petrovici, J. Schemmel, and K. Meier, “Versatile emulation of spiking neural networks on an accelerated neuromorphic substrate”, in *2020 IEEE International Symposium on Circuits and Systems (ISCAS)*, IEEE, Oct. 2020. DOI: 10.1109/iscas45731.2020.9180741.
- [18] S. Friedmann, J. Schemmel, A. Grübl, A. Hartel, M. Hock, and K. Meier, “Demonstrating Hybrid Learning in a Flexible Neuromorphic Hardware System”, *IEEE Transactions on Biomedical Circuits and Systems*, vol. 11, no. 1, pp. 128–142, 2017, ISSN: 1932-4545. DOI: 10.1109/TBCAS.2016.2579164.
- [19] J. Weis, P. Spilger, S. Billaudelle, Y. Stradmann, A. Emmel, E. Müller, O. Breitwieser, A. Grübl, J. Ilmberger, V. Karasenko, M. Kleider, C. Mauch, K. Schreiber, and J. Schemmel, “Inference with Artificial Neural Networks on Analog Neuromorphic Hardware”, in *Proceedings of the Workshop on IoT, Edge, and Mobile for Embedded Machine Learning (ITEM)/ECML-PKDD 2020 (submitted)*, Jun. 2020. arXiv: 2006.13177 [cs.NE].
- [20] J. Weis, “Inference with Artificial Neural Networks on Neuromorphic Hardware”, Master’s thesis, Universität Heidelberg, Sep. 2020.
- [21] A. Emmel, “Inference with Convolutional Neural Networks on Analog Neuromorphic Hardware”, Master’s Thesis, Universität Heidelberg, Nov. 2020.
- [22] P. Spilger, E. Müller, A. Emmel, A. Leibfried, C. Mauch, C. Pehle, J. Weis, O. Breitwieser, S. Billaudelle, S. Schmitt, T. C. Wunderlich, Y. Stradmann, and J. Schemmel, “hxtorch: PyTorch for BrainScaleS-2 — Perceptrons on Analog Neuromorphic Hardware”, in *Proceedings of the Workshop on IoT, Edge, and Mobile for Embedded Machine Learning (ITEM)/ECML-PKDD 2020 (submitted)*, Jun. 2020. arXiv: 2006.13138 [cs.NE].
- [23] G. D. Clifford, C. Liu, B. Moody, L.-W. H. Lehman, I. Silva, Q. Li, A. E. Johnson, and R. G. Mark, “AF Classification from a Short Single Lead ECG Recording: the PhysioNet/Computing in Cardiology Challenge 2017”, *Computing in Cardiology*, vol. 44, 2017, ISSN: 2325-8861 and 2325-887X.
- [24] D. E. Rumelhart, G. E. Hinton, and W. R.J., “Learning internal representations by error propagation”, *Parallel Distributed Processing: Explorations in the Microstructures of Cognition*, vol. I, D. E. Rumelhart and J. L. McClelland, Eds., pp. 318–362, 1986.
- [25] A. Paszke, S. Gross, F. Massa, A. Lerer, J. Bradbury, G. Chanan, T. Killeen, Z. Lin, N. Gimelshein, L. Antiga, A. Desmaison, A. Kopf, E. Yang, Z. DeVito, M. Raison, A. Tejani, S. Chilamkurthy, B. Steiner, L. Fang, J. Bai, and S. Chintala, “PyTorch: An Imperative Style, High-Performance Deep Learning Library”, in *Advances in Neural Information Processing Systems 32*, H. Wallach, H. Larochelle, A. Beygelzimer, F. d’Alché-Buc, E. Fox, and R. Garnett, Eds., Curran Associates, Inc., 2019, pp. 8024–8035. [Online]. Available: <http://papers.neurips.cc/paper/9015-pytorch-an-imperative-style-high-performance-deep-learning-library.pdf>.
- [26] S. Schmitt, J. Klähn, G. Bellec, A. Grübl, M. Güttler, A. Hartel, S. Hartmann, D. Husmann, K. Husmann, S. Jeltsch, V. Karasenko, M. Kleider, C. Koke, A. Kononov, C. Mauch, E. Müller, P. Müller, J. Partzsch, M. A. Petrovici, B. Vogginger, S. Schiefer, S. Scholze, V. Thanasoulis, J. Schemmel, R. Legenstein, W. Maass, C. Mayr, and K. Meier, “Classification With Deep Neural Networks on an Accelerated Analog Neuromorphic System”, *Proceedings of the 2017 IEEE International Joint Conference on Neural Networks*, 2017. DOI: 10.1109/IJCNN.2017.7966125. [Online]. Available: <http://ieeexplore.ieee.org/document/7966125/>.
- [27] I. Kacher, M. Portaz, H. Randrianarivo, and S. Peyronnet, “Graphcore c2 card performance for image-based deep learning application: A report”, *arXiv preprint*, Feb. 2020. arXiv: 2002.11670 [cs.CV].
- [28] B. Rueckauer, C. Bybee, R. Goettsche, Y. Singh, J. Mishra, and A. Wild, “NxTF: An API and Compiler for Deep Spiking Neural Networks on Intel Loihi”, *arXiv preprint*, Jan. 2021.
- [29] P. Spilger, “From Neural Network Descriptions to Neuromorphic Hardware — A Signal-Flow Graph Compiler Approach”, Master’s thesis, Universität Heidelberg, Feb. 2021.
- [30] G. M. Kurtzer, V. Sochat, and M. W. Bauer, “Singularity: Scientific containers for mobility of compute”, *PLOS ONE*, vol. 12, no. 5, pp. 1–20, May 2017. DOI: 10.1371/journal.pone.0177459.
- [31] T. Gamblin, M. LeGendre, M. R. Collette, G. L. Lee, A. Moody, B. R. de Supinski, and S. Futral, “The Spack Package Manager: Bringing Order to HPC Software Chaos”, in *Proceedings of the International Conference for High Performance Computing, Networking, Storage and Analysis*, ser. SC ’15, Austin, Texas: ACM, 2015, 40:1–40:12, ISBN: 978-1-4503-3723-6. DOI: 10.1145/2807591.2807623.
- [32] E. Müller, C. Mauch, P. Spilger, O. J. Breitwieser, J. Klähn, D. Stöckel, T. Wunderlich, and J. Schemmel, “Extending BrainScaleS OS for BrainScaleS-2”, *arXiv preprint*, Mar. 2020. arXiv: 2003.13750 [cs.NE].